

**INVESTIGATIONS ON A NEW HIGH-STRENGTH POZZOLAN
FOAM MATERIAL**

A Thesis
Presented to
The Academic Faculty

by

Julien Claus

In Partial Fulfillment
of the Requirements for the Degree
Master of Science in the
School of Civil and Environmental Engineering

Georgia Institute of Technology
December 2008

**INVESTIGATIONS ON A NEW HIGH-STRENGTH POZZOLAN
FOAM MATERIAL**

Approved by:

Dr. Mulalo Doyoyo, Advisor
School of Civil and Environmental Engineering
Georgia Institute of Technology

Dr. Kenneth M. Will
School of Civil and Environmental Engineering
Georgia Institute of Technology

Dr. Arash Yavari
School of Civil and Environmental Engineering
Georgia Institute of Technology

Date Approved: 11/11/08

To my family and my friends. Without their continuous support and guidance, I would not be here today.

ACKNOWLEDGEMENTS

I would like to thank my advisor, Dr. Doyoyo for all of his guidance, encouragement and support during the research. Through his guidance, my knowledge in civil engineering has increased immensely and has made me a better person. I also want to thank Dr. Will and Dr. Yavari for having accepted to be members of my thesis committee. Finally, I would like to express my gratitude to the Georgia Tech academic community, who helped me, not only for my research, but also in many aspects of my academic and professional life. It has been an extraordinary opportunity and a real pleasure to benefit by your vast knowledge and availability.

TABLE OF CONTENTS

	Page
ACKNOWLEDGEMENTS	iv
LIST OF TABLES	vi
LIST OF FIGURES	vii
SUMMARY	viii
<u>CHAPTER</u>	
1 INTRODUCTION	1
2 MATERIALS	7
3 UNIAXIAL EXPERIMENTS	11
Stiffness Measurements	11
Compressive Strength Measurements	16
Discussion	19
Influence of Chemical Composition	19
Influence of Particle Size	21
Influence of Curing Time	25
4 CONCLUSIONS	29
APPENDIX: Stress-strain curves in elastic range	30
REFERENCES	37

LIST OF TABLES

	Page
Table 1: 2006 Coal combustion products production and use in the United States	5
Table 2: 2005 coal consumption, CCP production and use in several countries	5
Table 3: Utilization and disposal of CCPs in Europe (EU 15) in 2003	5
Table 4: Chemical composition of different types of coal	7
Table 5: Chemical composition of CCPs used in the research: (A) cenospheres; (B) fly ash; (C) bottom ash	8
Table 6: Size range and distribution of cenospheres	8
Table 7: ASTM fly ash requirements	9
Table 8: Material curing conditions	11
Table 9: Physical and mechanical properties of material made up of Grade 500 cenospheres in SI units (A1) and standard units (A2)	20
Table 10: Physical and mechanical properties of material made up of Grade 500 cenospheres with new chemical compositions in SI units (A1) and standard units (A2)	20
Table 11: Physical and mechanical properties of material made up of the three types of cenospheres with chemical compositions 7 to 12 in SI units (A1) and standard units (A2)	22
Table 12: Physical and mechanical properties of material made up of: fly ash C in SI units (A1) and standard units (A2); fly ash F in SI units (B1) and standard units (B2); bottom ash in SI units (C1) and standard units (C2)	24
Table 13: Mechanical properties of the new materials and of three lightweight concretes in SI units (A1) and standard units (A2)	25
Table 14: Compressive strength increase due to the addition of 0.5g of aluminum phosphate for CG106-9 after 1h, 2h30, 4h and 5h30 of curing	28

LIST OF FIGURES

	Page
Figure 1: Various specimens based on: (a) Grade 500LF cenospheres; (b) Grade 500 cenospheres, (c) Grade 106 cenospheres, (d) fly ash C, (e) fly ash F, (f) bottom ash	11
Figure 2: Signal form from the test for the determination of the Young's Modulus	12
Figure 3: Typical stress-strain curve in the elastic range	13
Figure 4: Stress-strain curves in elastic range for: (a) CG500-11; (b) CG500LF-11; (c) CG106-11	14
Figure 5: Stress-strain curves in elastic range for: (a) CC-11; (b) CF-11; (c) CB-11	15
Figure 6: Signal form from the test for the determination of the compressive strength	16
Figure 7: Typical stress-strain curve in the plastic range	17
Figure 8: Material' failure through vertical cracks - example of CF-12 specimen	17
Figure 9: Stress-strain curves in plastic range for: (a) CG500-1; (b) CG500-2; (c) CG500-3; (d) CG500-4	18
Figure 10: Primary (red) and secondary (blue) paste compositions used to investigate the influence of chemical composition on the compressive modulus and compressive strength	19
Figure 11: Simplified model showing the optimized arrangement of circular particles within a plan	22
Figure 12: Strength vs. Aluminum phosphate quantity for CG106-9 after a curing of: (1) 1h; (2) 2.5h; (3) 4h; (4) 5.5h	27

SUMMARY

This thesis describes improvements on newly-discovered high-strength pozzolan-based materials fabricated via a low-cost chemical reaction that takes place between 90 and 115 °C for 3 to 24 hours. The reported results focus on pozzolan constituents acquired from Coal Combustion Products (CCPs) such as cenospheres, fly ash C and F, as well as bottom ash. The thesis reports on various types of these materials with specific gravity ranging from 0.5 to 1.6; compressive strength ranging from 300 to 3600 psi, and compressive modulus ranging from 50 to 240 ksi. In addition to their good mechanical properties under compression that are attractive for the building and construction industries, the materials further exhibit great potential for applications as energy absorption cores in sandwich construction that could extend their value in other industries including the automotive and aerospace industries. For example, the load-displacement curve exhibits a short elastic zone followed by a long load-plateau; while the materials crush through a controlled vertical cracking process. Additionally, an attempt was made to further decrease the manufacturing cost of the material by investigating incorporation of chemicals that accelerates dehydration of the mixture. One such successful chemical reported in this thesis is aluminum phosphate; while it is not conclusive how the chemical improves any major property.

CHAPTER 1

INTRODUCTION

In a world where sustainability has become commercially viable, building and construction industries have to adapt and respond to the changing societal-driven regulations. It is, for example, being increasingly considered environmentally-responsible to attempt to reduce the excessive consumption of virgin raw materials by traditional construction materials such as concrete, wood, and asphalt. Also, as one of the major carbon dioxide emitting processes, calcination that is used in cement production has inspired a movement towards the lowering of the amount of cement in concrete. Numerous investigations continue to create social awareness that cement manufacturing has non-negligible negative environmental impacts. The negative environmental effects caused by the cement industry are covered by numerous publications (e.g. Malhotra, 2005, ACI Board Advisory Committee on Sustainable Development, 2005). It has been proven for instance that the heating of calcium carbonate during calcination releases significant amounts of carbon dioxide into the atmosphere. Some estimates project that the cement industry emits nearly 900 kg of CO₂ for every 1000 kg of cement produced (Mahasenan and Smith, 2003). It has been stated that the cement industry is responsible for the release of 5% of the total man-made CO₂ into the atmosphere (World Business Council for Sustainable Development, 2002). Moreover, the calcination process occurs at elevated temperatures and therefore requires significant energy which is mainly provided by fossil fuels, such as coal and petroleum.

In a similar context, the logging of trees for timber, mining, biofuels and infrastructure development reduces the earth's capacity to absorb carbon dioxide. Indeed, via photosynthesis, trees are able to convert carbon dioxide into oxygen thereby contributing to the maintenance of atmospheric equilibrium (Singhal and Renger, 2006).

By reducing tree densities around the globe through timber mining and other forms of deforestation, nature's capability to absorb CO₂ is highly compromised. A little more than a decade ago, some experts claimed that deforestation only had a minor effect on global warming (Moran, 1993); but with the emergence of the Big Emerging Markets and accelerated development that go hand in hand with forest removal, such claims may be outdated. For example, in a recent study; it was shown that the incineration of trees as a means of forest clearance for construction, however, releases, in a much more direct way, substantial amounts of CO₂ (Fearnside and Laurance, 2004). In addition, massive wood utilization leading to deforestation for construction purposes has dramatic negative environmental impacts on biodiversity. As a matter of fact, countless species disappear every day during the deforestation process (WWF, 2008).

Furthermore, nowadays, most of the roads in developed countries are made of asphalt which is an oil-based material. The manufacturing process of this material causes the release of toxic gases into the atmosphere during fossil fuel burning and is responsible for the consumption of virgin materials such as stone aggregates, sand, and crude oil. There exists a need for a new material in the building and construction industries which could exhibit good mechanical properties and whose manufacturing and operational process would be sustainable and environmentally-friendly. The concept of green building and green construction has soared in modern times. What makes a building "green" is essentially its location, its energy source, its construction materials, and its water efficiency. Several studies have outlined the benefits of green construction. For instance, it has been demonstrated that sustainable buildings have positive effects on the occupants' health by decreasing the risk of respiratory problems, as well as increasing their general productivity. There are also some economic benefits; while green buildings may be more costly than traditional buildings in the beginning, their low operating costs make them cheaper than regular building over time (Ries and Bilec, 2006, Paul and Taylor, 2008). The US Green Building Council has developed a means of evaluating the

degree of “greenness” of a project or building. This is known as the Leadership in Energy and Environmental Design (LEED) green building rating system. The LEED designation has been nationally accepted and is now respected by the entire profession. As far as energy needs are concerned, a material has to limit thermal transfer for better energy efficiency in order to be certified as a “green material”. In addition, several other criteria have been developed. For instance, the material used must be recyclable in order to reduce waste, it must limit the disruption of natural water flow, and its transportation and manufacturing must have low environmental impacts. Recently, the development of a potential green competitor to concrete has been the subject of numerous investigations by taking advantage of the pozzolanic reaction [ASIDE: A pozzolan is a material which can combine with calcium oxide to exhibit cementitious properties]. The general aim is usually to partially replace cement with some pozzolan materials such as fly ash, granulated blast furnace slag, condensed silica fume, or rice hull ash (Tanyildizi and Coskun, 2008, Yazici and Yigiter, 2008). However, strong and competitive building and construction materials that do not contain cement at all remain rare.

For example, the attempt of replacing a part of the brick clay (mixture of clay and sand) with fly ash in bricks has not convinced the masonry community yet. In a study performed in 2001 (Fatih, 2001), it was concluded that the addition of fly ash had no significant harmful effects on the brick quality but no improvement was witnessed. Bricks were manufactured by the autoclaving method at the molding pressure of 4350 psi (30 MPa or 296 atm) at temperatures of 750, 850 and 950°C. Bricks containing 50 and 60% fly ash in mass had relatively low compressive strength (6 to 11 MPa or 870 to 1600 psi) with specific gravities ranging from 1.31 to 1.38. In addition, Fatih observed that fly ash bricks tended to fail unexpectedly in a high moisture environment, due to a chemical reaction which caused bricks to expand. Finally, other issues, such as a low resistance to abrasion or fire, occurred. However, in 2007, a new generation of fly ash bricks has been presented to the masonry committee (Liu, 2007): based on fly ash C and water only, the

new bricks require to be cured for 24 hours in a 66 °C steam bath at a pressure of 4,000 psi (28 MPa or 272 atm). Due to the current licensing of the discovery, no data concerning the bricks weight (although the specific gravity of fly ash C is reported to range from 2.1 to 3) and strength are available at present.

Coal Combustion Products (CCPs) are by-products of the combustion of coal in electric power plants. They can be classified into four categories: fly ash, bottom ash, flue gas desulfurization (FGD) materials and boiler slag. In 2006, 113.2 million of tons of CCPs were produced in the United States, 43% of which were used beneficially while the rest were disposed (American Coal Ash Association, 2006)(Table 1), mainly into landfills and storage lagoons. Much of this ash is, however, capable of being recovered and used, which makes it an almost inexhaustible raw material for new applications. In developing countries such as India, coal combustion remains the most common source of electricity. The coal used in India (mainly bituminous and sub-bituminous) is usually of low-quality and contains over 40% ash. Such circumstances result in the production of huge amounts of fly ash (more than 180 million of tons per year) and the country is desperately looking for a way to use it economically (Mukherjee and Zevenhoven, 2006) (Table 2). In South Africa, although the country has come to realize the importance of the use of CCPs and started to use fly ash to manufacture blended cements and as a supplementary cementitious material in concrete, the quantity of fly ash reused remains negligible and bottom ash is practically unused at present (SACAA, 2008) (Table 2). In Europe (EU 15), the reuse of coal ash is more common, 65 million tons of CCPs were produced in 2003 (European Coal Ash Association, 2003), around half of which had an application in the construction industry and in underground mining (Table 3).

Table 1: 2006 Coal combustion products production and use in the United States (ACAA, 2006)

CCP	Fly Ash	Bottom Ash	Flue Gas Desulfurization	Boiler Slag	Total
Production (Mt)	65.7	16.9	28.8	1.8	113.2
Usage (Mt)	29.4	7.6	10.6	1.5	49.1
% Usage	45	45	37	83	43

Table 2: 2005 coal consumption, CCP production and use in several countries (ACAA, ECOBA, SACAA, World Energy Council, Mukherjee and Zevenhoven, 2006)

Country	Coal Consumption (Mt)	CCP released (Mt)	% CCP reused	% CCP reused in construction
USA	1021	112	40	36
Europe (15)	520	65	89	52
South Africa	174	47	10	>8
India	450	> 180	2	/

Table 3: Utilization and disposal of CCPs in Europe (EU 15) in 2003 (ECOBA, 2003)

	Construction Industry and Underground Mining	Restoration of Open Cast Mines, Quarries and Pits	Temporary Stockpile	Disposal	Total
CCP used (Mt)	34.1	23.3	5.2	2.4	65
% CCP used	52.4	35.9	8	3.7	100

CCPs have a wide range of applications in the construction industry; they can be used as a replacement for Portland cement, as aggregates, as embankments, structural fill, or as blasting grit. CCPs can also be used to stabilize soft soils, or they can be used in ice and snow control. In particular, the use of fly ash as a partial replacement for Portland cement is generally limited to Class F fly ash. It can replace up to 30% of the mass of Portland cement and can add to concrete's final strength, as well as increase its chemical resistance and durability. Concrete based on fly ash-cement can therefore contain up to 15% fly ash by volume. A massive use of CCPs would lead to the recovery of millions of acres of land currently used for CCP disposal. In the construction field, the use of fly ash as a replacement for cement would lead to a significant decrease of CO₂ released in the atmosphere during the cement manufacturing process (Mahasenan and Smith, 2003, Malhotra, 2005).

This thesis presents additional investigations on a high-strength material that is completely cement-free, which uses pozzolan particles from coal combustion products as aggregates and is manufactured without autoclaving. Since the material uses pozzolans as aggregates while being as strong as concrete, it promises a more sustainable and environmentally-friendly alternative to concrete.

CHAPTER 2

MATERIALS

A new series of lightweight materials based on CCPs has recently been discovered and will be presented in this thesis. These new aluminosilicates are based on natural pozzolanic materials. The different materials contain from 50% to 80% of CCPs by volume, exhibit excellent physical properties including lightweight, high strength and excellent sound and thermal insulation properties. The coal ashes are predominantly made up of four constituents: SiO_2 , Al_2O_3 , Fe_2O_3 and CaO . The relative quantity of each constituent depends essentially upon the coal which produced the ashes (Table 4). The use of three types of cenospheres (Grade 500, 500LF, 106), the use of fly ash C and F, and the use of bottom ash as pozzolan particles will be presented in this thesis.

Table 4: Chemical composition of different types of coal

Coal	Bituminous	Sub-Bituminous	Lignite
% SiO_2	20-60	40-60	15-45
% Al_2O_3	5-35	20-30	20-25
% Fe_2O_3	10-40	4-10	4-15
% CaO	1-12	5-30	15-40

Cenospheres are lightweight (0.35-0.45g/cc), hollow and spherical microspheres, which can be extracted from fly ash. The cenospheres used in the research were provided by Trelleborg Fillite Ltd, the world's largest supplier of cenospheres. The three types of cenospheres used in the research have the same chemical properties which are tabulated in Table 5. The cenospheres only differ in the particle size range and distribution (Table 6).

Table 5: Chemical composition of CCPs used in the research: (A) cenospheres; (B) fly ash; (C) bottom ash

SiO ₂	Al ₂ O ₃	Fe ₂ O ₃	K ₂ O	Na ₂ O	CaO	MgO	TiO ₂
55-65%	27-33%	6% max	5%	1%	0.5%	1.5%	1%

(A)

	Chemical Composition								
	SiO ₂ %	Al ₂ O ₃ %	Fe ₂ O ₃ %	CaO %	MgO %	SO ₃ %	Na ₂ O %	K ₂ O %	Others %
Fly Ash C	35.78	17.67	6.14	25.58	6.22	2.23	1.84	0.48	4.06
Fly Ash F	53.51	26.86	8.52	1.41	1.08	0.17	0.45	3.12	4.88

(B)

SiO ₂	Al ₂ O ₃	Fe ₂ O ₃	MgO	CaO	Na ₂ O	K ₂ O
45 - 55 %	20 - 30 %	5 - 15 %	2 - 5 %	0 - 2 %	0 - 1 %	0 - 1 %

(C)

Table 6: Size range and distribution of cenospheres

Cenospheres Grades	500	500 LF	106
Particle Size Range (microns)	5-500	5-500	5-106
Particle Size Distribution			
% Passing 500 microns	100	100	100
% Passing 300 microns	85-100	97-100	100
% Passing 150 microns	40-80	40-60	100
% Passing 106 microns	25-55	15-30	99.7-100
% Passing 50 microns	2-10	2-10	15-30

Fly ash is the most available CCP. In the past, fly ash was released into the atmosphere, but new pollution regulation laws now require that each plant built in the US be equipped with a system for collecting and stocking fly ash. Fly ash particles are generally spherical in shape, either solid or hollow, amorphous and range in size from 0.5 μm to 100 μm. The fly ash specific gravity ranges from 2.1 to 3.0 and a dry unit specific gravity ranges from 0.6 to 1.7. To be used in concrete applications, the fly ash must meet ASTM C 618 requirements. These include material processing requirements such as source control (the ash from a peaking plant may not, for instance, be used instead of the

ash coming from a base loaded plant), drying or conditioning, quality control and some engineering properties: the fineness (maximum of 34 % retained in a 0.045 mm sieve), the loss on ignition (it corresponds to the change of mass of the material when strongly heated; this mass modification is due to the release of volatile substances trapped into the material), the moisture content (Table 7). In addition, workability, setting time, pumpability, strength development, heat of hydration, permeability, resistance to freeze-thaw and the sulfate resistance are also controlled. ASTM C 618 differentiates two types of fly ash - C and F - mainly according to chemical composition. Fly ash is made of four main constituents: silicon dioxide SiO_2 , aluminum oxide Al_2O_3 , iron oxide Fe_2O_3 and calcium oxide CaO . Table 7 is a partial list of the requirements for fly ash to be used in concrete.

Table 7: ASTM fly ash requirements (ASTM C 618, 2008)

Properties	Fly Ash Class	
	Class C	Class F
$(\text{SiO}_2 + \text{Al}_2\text{O}_3 + \text{Fe}_2\text{O}_3)\text{min, \%}$	50	70
Sulfur trioxide (SO_3), max, %	5	5
Moisture Content, max, %	3	3
Loss on ignition, max, %	6	6

The fly ash used in this study has been provided by Boral Material Technologies. Fly ash F comes from the Bowen Power Plant located in Cartersville, GA, while fly ash C comes from the Scherer Power Plant located in Juliette, GA. According to tests performed by Boral on some samples in April and May 2008, the chemical properties of the fly ash used in the research are tabulated in Table 5.

Bottom ash is a coarse by-product of steam generation, which is collected from the bottom of furnaces. The bottom ash specific gravity ranges from 2.1 to 2.7 and a dry unit specific gravity ranges from 0.7 to 1.6 Typically, the bottom ash particle size ranges from 0.01 mm to 40 mm and only 10 to 60 percent of the particles would pass through a

0.42 mm (No.40) sieve. The Bottom Ash was also provided by the Plant Bowen which is one of the biggest power plants in the US, with a power generation of 22,630,000 MWh in 1998. Its chemical composition is listed in Table 5.

All the specimens except those based on fly ash C have a color ranging from pale grey to dark grey, while the relatively high content of calcium oxide in fly ash C provides the material with a cream color aspect (Fig. 1). All specimens have a fine texture with the exception of those based on bottom ashes which are coarse aggregates. The material used in this study is based on the ash bonded together by a cementitious slurry; the ash provides the material with high strength while the slurry gives some coherence to the material by bonding the ash particles together. The chemical composition of the slurry is directly linked with some physical properties of the material such as its strength or its weight. Different chemical compositions have been investigated in the research. Various curing conditions have been applied to the specimens as shown in Table 8.

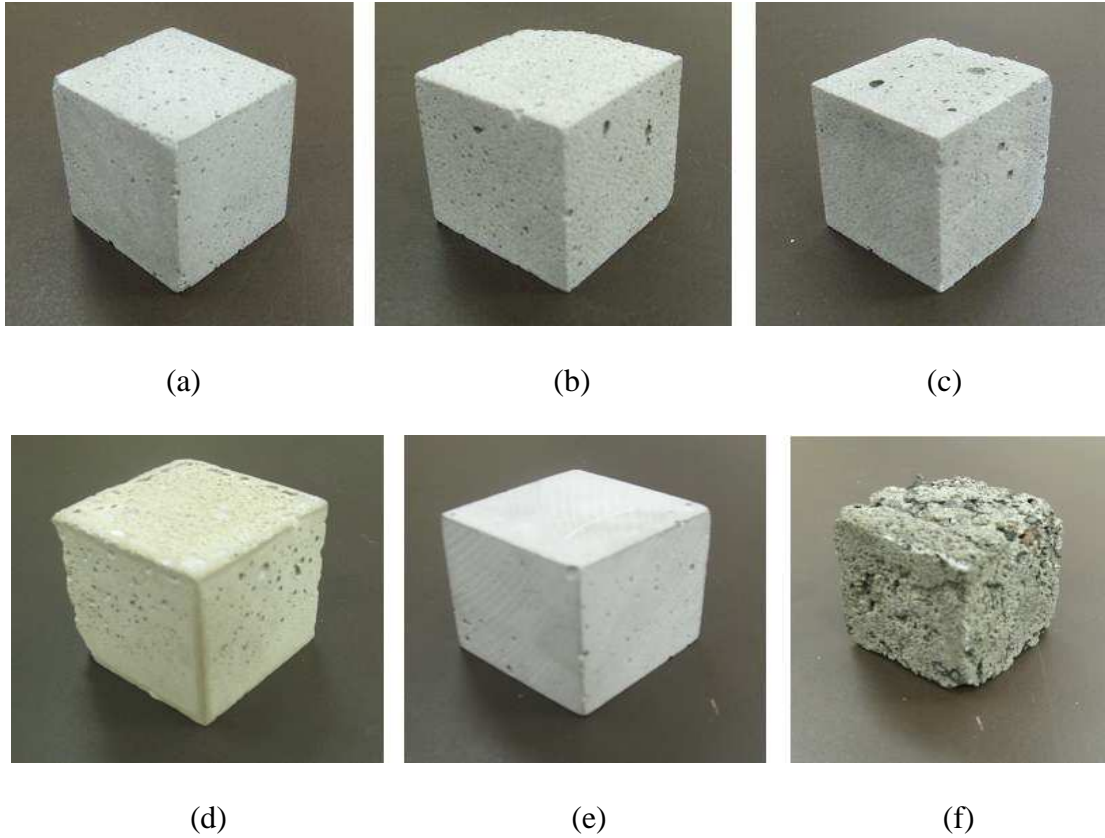


Figure 1: Various specimens based on: (a) Grade 500LF cenospheres; (b) Grade 500 cenospheres, (c) Grade 106 cenospheres, (d) fly ash C, (e) fly ash F, (f) bottom ash

Table 8: Material curing conditions

	Curing Time (hours)	Curing Temperature (°C)
Cenospheres	24	115
Fly Ash C	3.5	90
Fly Ash F	24	115
Bottom Ash	24	115

Due to the high number of tests performed, we will use the same nomenclature throughout the paper: a specimen called CG500-2 will refer to a material made up of Grade 500 cenospheres and from chemical composition 2 while CF-9 will refer to a material made up of fly ash F and from chemical composition 9.

CHAPTER 3

UNIAXIAL EXPERIMENTS

Stiffness Measurements

Uniaxial compression tests have been performed on several specimens of different compositions and porosity. All the samples were 2''x 2''x 2'' cubes and were manufactured with a bronze cube mold. The mold was composed of a base and a top plate to insure homogeneous heating. This mold conforms to specifications ASTM C 87, C 109, C 141, C 257, C 267, C 306, C 472, C 379, C 396, and AASHTO T-106. The experimental tests have been accomplished using an Instron 8802 displacement-controlled testing machine. Two tests have been performed in order to evaluate the mechanical properties in compression. The first test aims to determine the compressive Young's Modulus of the material and its evolution throughout the different stages of its deformation. We first loaded and unloaded the specimen at a constant deformation rate of 0.16mm/sec staying in the elastic range (Fig. 2).

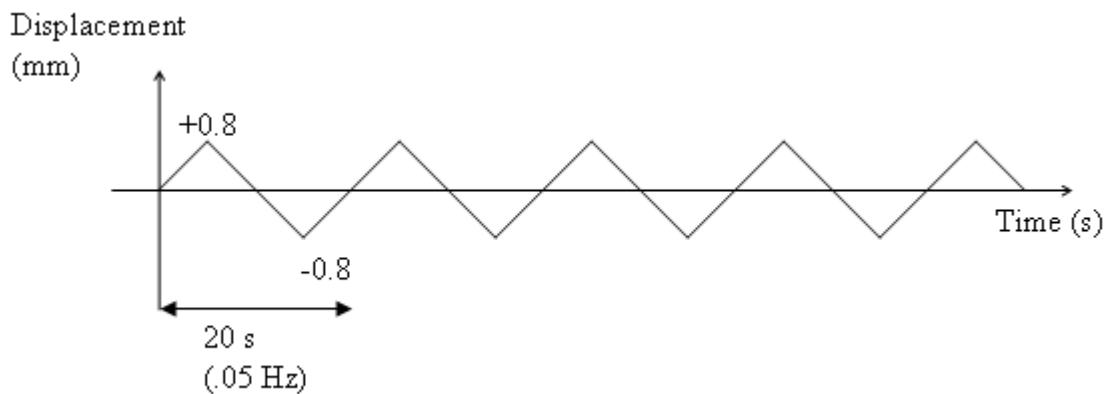


Figure 2: Signal form from the test for the determination of the Young's Modulus

The typical stress-strain curve in the elastic range is given in figure 3. We can observe a first cycle where the slope of the curve is low. It corresponds to a hardening process of the material, during which it will reach its full stiffness (1). Then all the following cycles have a similar slope, corresponding to the compressive Young's modulus of the material (2). This Stress vs. Strain curve is typical of cellular materials. During the first compressive cycle, the air pockets get progressively closed, plus there is a microscopic reorganization of the particles which leads to a stiffer material.

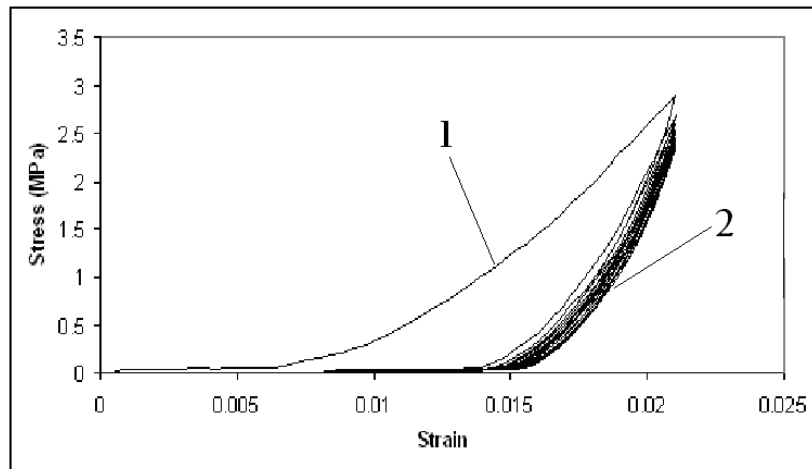
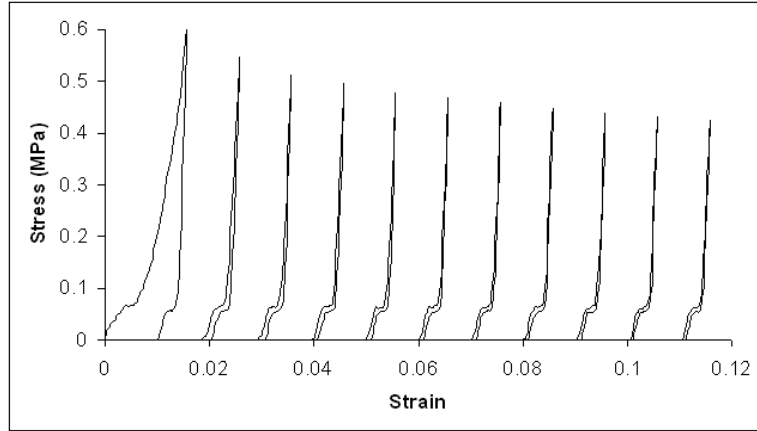
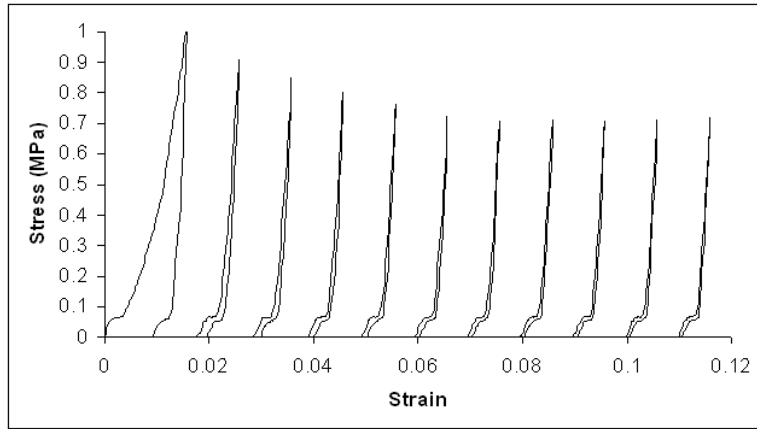


Figure 3: Typical stress-strain curve in the elastic range

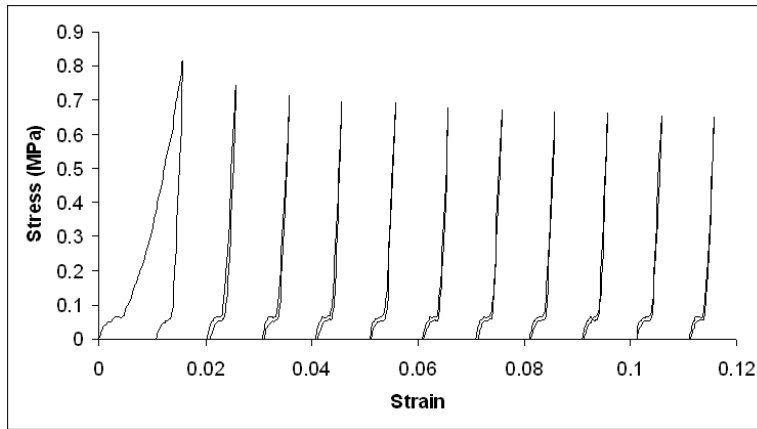
The stress-strain curve represented in Figure 3 is the actual response of the material. This curve is difficult to interpret since all the cycles are superimposed. Another curve, which decomposes the different cycles of the response by adding an artificial strain between each cycle, can be drawn for the analysis, as shown on Figures 4 and 5. The Figures 4 and 5 represent the stress-strain curves for chemical composition 11 and for each type of aggregates. For the totality of the curves, please refer to the appendix. The results are presented and discussed later in the thesis.



(a)

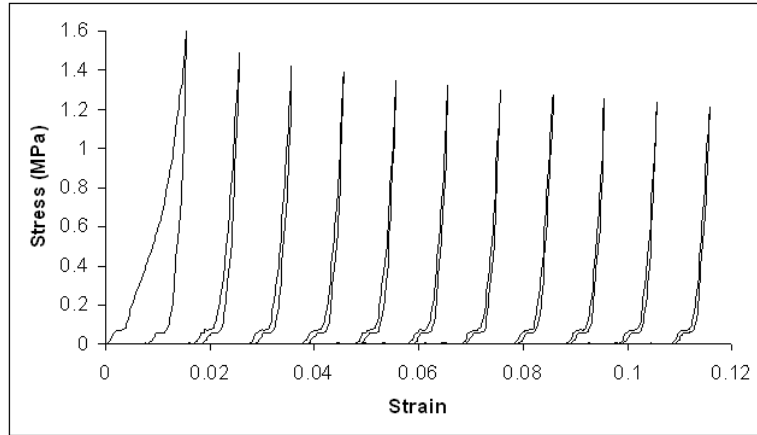


(b)

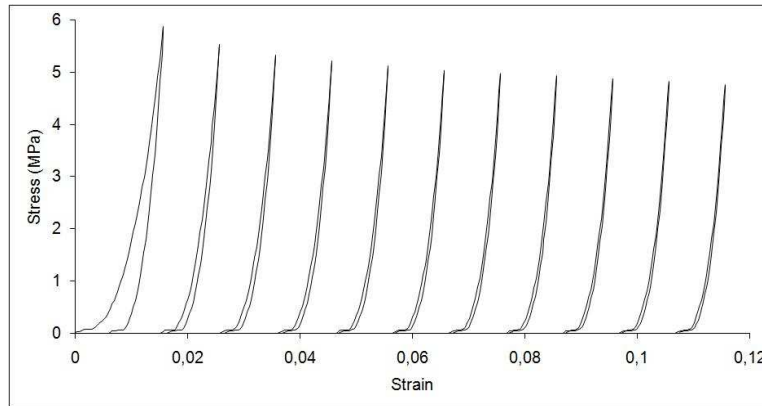


(c)

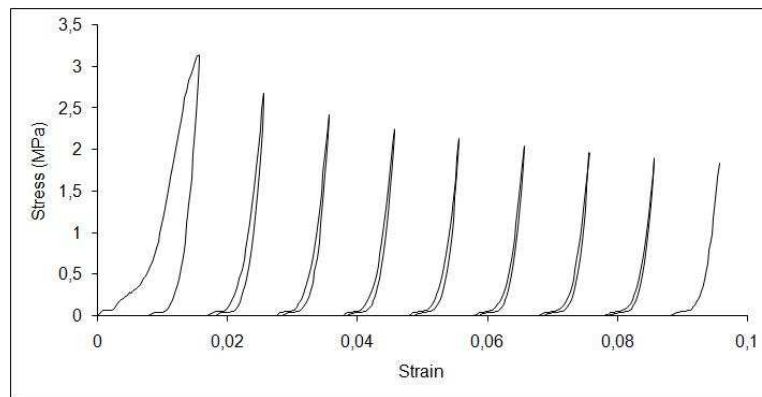
Figure 4: Stress-strain curves in elastic range for: (a) CG500-11; (b) CG500LF-11; (c) CG106-11



(a)



(b)



(c)

Figure 5: Stress-strain curves in elastic range for: (a) CC-11; (b) CF-11; (c) CB-11

Compressive Strength Measurements

A second test has been performed subsequently on the same specimens: we loaded and unloaded the specimens with increasing displacement amplitude keeping the deformation rate around 0.2mm/sec (Fig. 6). The second test was performed until complete failure of the material and revealed the compressive strength of the material.

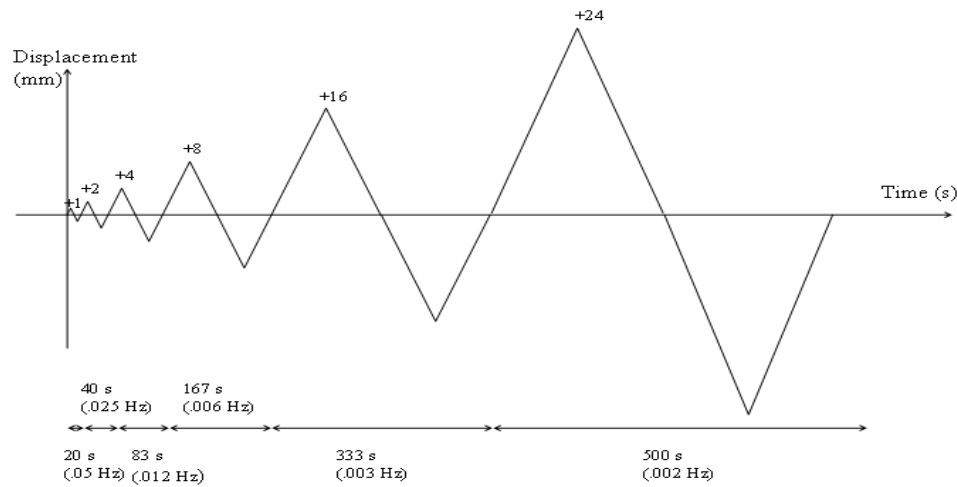


Figure 6: Signal form from the test for the determination of the compressive strength

The typical stress-strain curve in the plastic range is represented in Figure 7. We can observe a first linear part corresponding to the elastic range (1) until a maximum stress (compressive strength) is reached. Then, a decrease of the strength occurs, followed by a wide horizontal plateau (3), typical of high energy absorber material. Finally, there is a zone of densification (4). Initially, the material undergoes reversible deformation until a first vertical crack, due to the Poisson' effect, appears (Fig.8). Then the strength of the material decreases until it reaches a plateau and stabilizes. Along the plateau, the cenospheres get crushed and the air pockets get progressively rarer. The densification is due to the fact that our material has a cellular structure. Indeed, under high stresses, the cells will independently fail and a densification phenomenon will occur.

The stress value corresponding to the end of the elastic part and the average stress value of the plateau are critical. The former, known as compressive strength, shows how much load can be applied before the material undergoes permanent deformation (2). The latter has a key role in the energy absorption properties. The area under the stress-strain curve is indeed proportional to the energy that can be absorbed by the material.

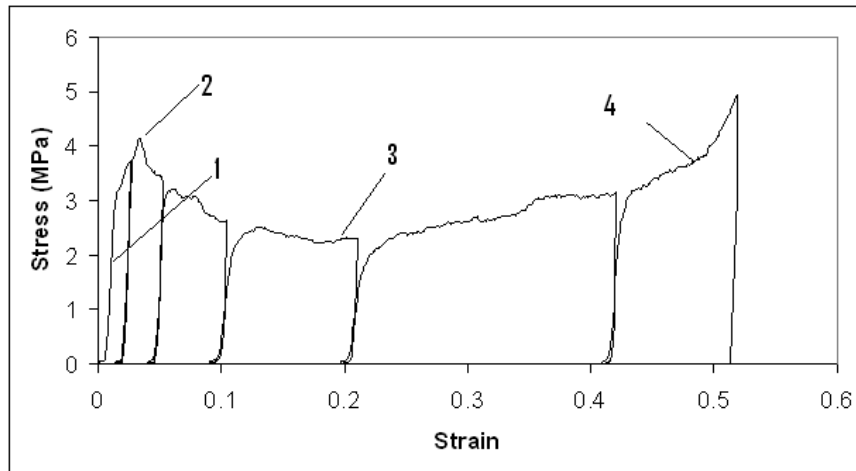


Figure 7: Typical stress-strain curve in the plastic range

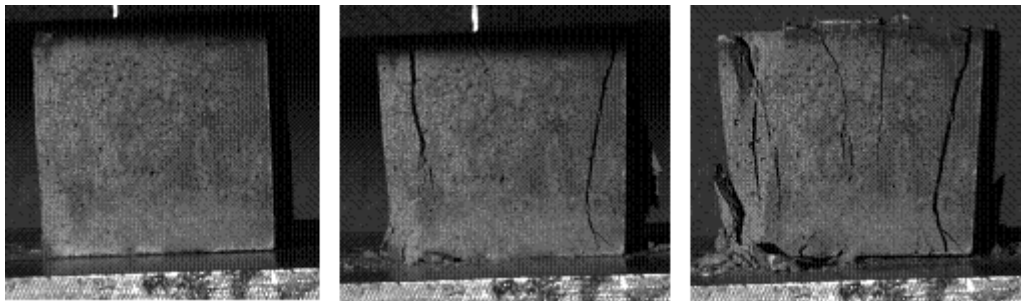
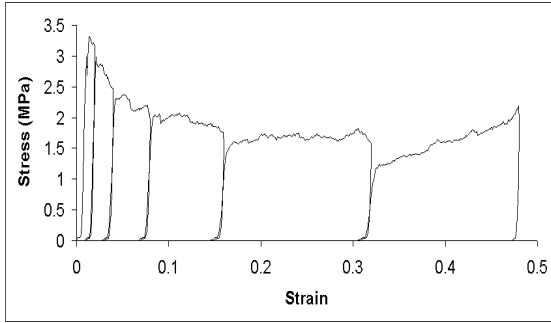
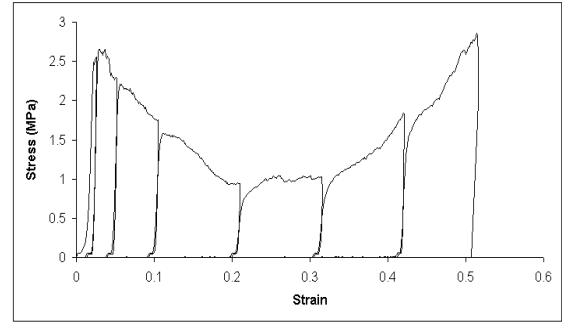


Figure 8: Material' failure through vertical cracks - example of CF-12 specimen

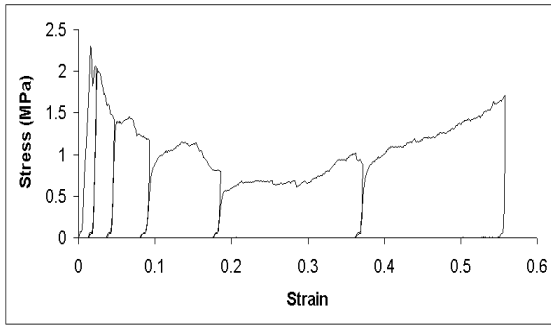
The stress-strain curves for CG500-1 to CG500-4 specimens in the plastic range are represented in Figure 9.



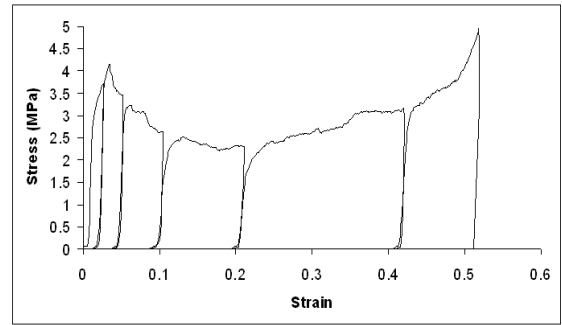
(a)



(b)



(c)



(d)

Figure 9: Stress-strain curves in plastic range for: (a) CG500-1; (b) CG500-2; (c) CG500-3; (d) CG500-4

Discussion

Influence of Chemical Composition

Some investigations had already been performed on the material made up of grade 500 cenospheres (Paul Biju-Duval, 2006). Nevertheless, the compressive properties have been reinvestigated with the testing protocol described earlier. Below, the ternary diagram shows all the chemical compositions which had been primarily investigated (Fig.10) and also the results obtained for the grade 500 cenospheres with the new testing protocol (Table 9). Chemicals C1, C2 and C3 can not be identified in this thesis as they are treated by intellectual property.

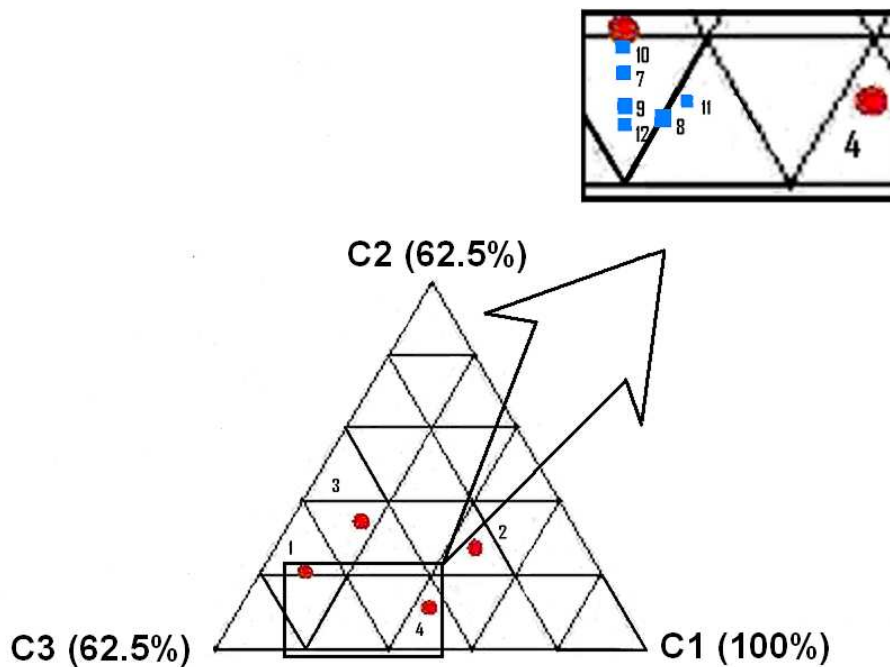


Figure 10: Primary (red) and secondary (blue) paste compositions used to investigate the influence of chemical composition on the compressive modulus and compressive strength

Table 9: Physical and mechanical properties of material made up of Grade 500 cenospheres in SI units (A1) and standard units (A2)

Specimen	Specific Gravity	Compressive Modulus (GPa)	Compressive Strength (Mpa)
CG500-1	0.54	0.57	2.93
CG500-2	0.57	0.60	2.35
CG500-3	0.53	0.49	2.49
CG500-4	0.57	0.73	3.94

(A1)

Specimen	Specific Gravity	Compressive Modulus (ksi)	Compressive Strength (psi)
CG500-1	0.54	82	424
CG500-2	0.57	87	340
CG500-3	0.53	71	360
CG500-4	0.57	106	571

(A2)

CG500-1 and CG500-4 specimen have the best mechanical properties: they exhibit greater compressive strength and compressive modulus than the other specimens. We have therefore decided to narrow the ternary diagram around these two compositions in order to reduce our area of study. In the previous diagram (Fig. 10), six new chemical compositions intended to approach the optimal chemical composition are represented. The same testing protocol has been repeated for the specimens made up of Grade 500 cenospheres with the six new chemical compositions. The results are listed in Table 10. Even though there is no major improvement in the compressive modulus and the specific gravity, we can observe a significant increase in compressive strength with the new chemical compositions: 2.6-6.5 MPa (370-940 psi) versus 2.3-3.9 MPa (340-570 psi). In the reminder of the thesis, only the six new chemical compositions will be investigated.

Table 10: Physical and mechanical properties of material made up of Grade 500 cenospheres with new chemical compositions in SI units (A1) and standard units (A2)

Specimen	Specific Gravity	Compressive Modulus (GPa)	Compressive Strength (Mpa)
CG500-7	0.50	0.40	3.04
CG500-8	0.57	0.51	2.57
CG500-9	0.59	0.37	5.07
CG500-10	0.57	0.56	3.37
CG500-11	0.64	0.43	3.68
CG500-12	0.62	0.60	6.51

(A1)

Specimen	Specific Gravity	Compressive Modulus (ksi)	Compressive Strength (psi)
CG500-7	0.50	58	441
CG500-8	0.57	74	373
CG500-9	0.59	54	735
CG500-10	0.57	81	489
CG500-11	0.64	62	534
CG500-12	0.62	87	944

(A2)

Influence of Particle Size

In this section, the influence of particle size on the mechanical properties of the material will be demonstrated. The three types of cenospheres (grade 500-500LF -106) used in the research have identical chemical properties, which are tabulated in Table 5. The cenospheres differ only in their particle size range and distribution (Table 6). The following example highlights the influence of the particle size on the total surface area. If we consider two spherical particles whose radius are r and $2r$; along a line of a given dimension, there are twice as many small particles of radius r as large particles of radius $2r$. Inside a rectangle of a given dimension, there are $2^2=4$ times more small particles than large particles (as shown in Figure 11). And eventually within a parallelepiped, there are $2^3=8$ times more small particles than large particles. If N represents the number of particles inside a parallelepiped of a given size, the total surface area available inside this parallelepiped for the large particles is: $S_{\text{large}} = 16N\pi r^2$. On the other hand, the total surface area available inside the same parallelepiped for the small particles is: $S_{\text{small}} = 32N\pi r^2$. The available surface area for the small particles is then twice as great as the surface area available for the large particles. Chemical reactions can then take place in a larger area if small particles are used. This results in a better bond between the cenospheres and, therefore, in a stronger material. In order to validate this model, the relationship of particle size to mechanical properties of the material is tabulated below (Table 11), together with the compressive strength and modulus of the new material made up of each type of cenosphere.

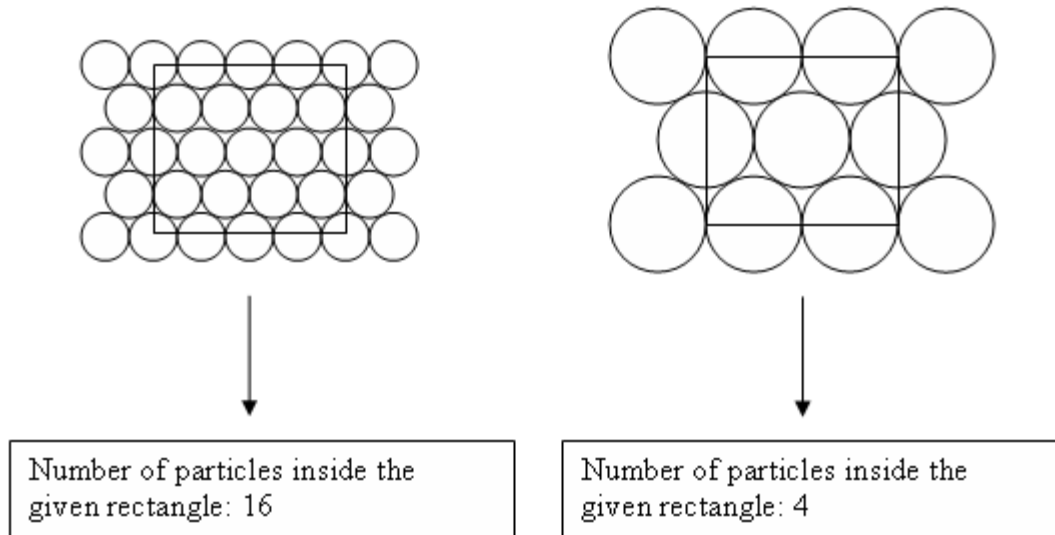


Figure 11: Simplified model showing the optimized arrangement of circular particles within a plan

Table 11: Physical and mechanical properties of material made up of the three types of cenospheres with chemical compositions 7 to 12 in SI units (A1) and standard units (A2)

Specimen	Specific Gravity	Compressive Modulus (GPa)	Compressive Strength (Mpa)
CG500LF-7	0.54	0.66	3.14
CG500LF-8	0.55	0.79	3.35
CG500LF-9	0.57	0.60	3.81
CG500LF-10	0.48	0.52	2.72
CG500LF-11	0.57	0.55	3.42
CG500LF-12	0.57	0.50	3.16
CG500-7	0.50	0.40	3.04
CG500-8	0.57	0.51	2.57
CG500-9	0.59	0.37	5.07
CG500-10	0.57	0.56	3.37
CG500-11	0.64	0.43	3.68
CG500-12	0.62	0.60	6.51
CG106-7	0.58	0.62	8.10
CG106-8	0.55	0.38	8.56
CG106-9	0.55	0.46	7.05
CG106-10	0.58	0.51	9.63
CG106-11	0.54	0.42	5.56
CG106-12	0.60	0.60	11.64

(A1)

Specimen	Specific Gravity	Compressive Modulus (ksi)	Compressive Strength (psi)
CG500LF-7	0.54	96	455
CG500LF-8	0.55	114	486
CG500LF-9	0.57	87	553
CG500LF-10	0.48	75	395
CG500LF-11	0.57	80	496
CG500LF-12	0.57	73	458
CG500-7	0.50	58	441
CG500-8	0.57	74	373
CG500-9	0.59	54	735
CG500-10	0.57	81	489
CG500-11	0.64	62	534
CG500-12	0.62	87	944
CG106-7	0.58	91	1175
CG106-8	0.55	55	1242
CG106-9	0.55	67	1023
CG106-10	0.58	74	1397
CG106-11	0.54	61	806
CG106-12	0.60	87	1688

(A2)

All the specimens made up of cenospheres have a similar specific gravity ranging from 0.48 to 0.64 and similar compressive modulus ranging from 0.37 to 0.79 MPa (53 to

114 ksi). However, the specimens made up of Grade 106 cenospheres exhibit greater Compressive Strength than those made of Grade 500 and 500LF cenospheres: 5.6 to 11.6 MPa (810 to 1690 psi) versus 2.6 to 6.5 MPa (370 to 740 psi).

If light weight is not a major concern, other CCPs can be used as replacement for cenospheres. Given that the cenospheres, fly ash F and the bottom ash come from the same coal, their chemical compositions are almost identical (Table 7). Fly and bottom ash particles are mainly solid instead of being hollow as in the case for the cenospheres, which makes them slightly heavier. Moreover, as it has already been stated earlier in the thesis, the bottom ash particle size and distribution differs significantly from the fly ash particle size and distribution. Following the same manufacturing process, various specimens based on fly ash C or F have been produced and the behaviors of the different series of material have been investigated (Table 12). One major difference between the two types of fly ash is that the chemistry of the reaction is not the same in both cases. Firstly, for fly ash C, two reactions occur in a parallel way: the formation of calcium silicate hydrate (C-S-H), commonly called hydration, and the classic aluminosilicate transformation, which is the main reaction taking place in the material. The production of C-S-H, responsible for the strength in cement based materials, is made possible thanks to the high ratio of calcium oxide in this type of fly ash. Indeed, the silica and alumina from the fly ash, which are pozzolans, do not need any external provision of calcium oxide and can combine directly with the calcium oxide already present in the fly ash to form a cementitious material. The second reaction is due to the combined action of the three chemicals on the fly ash. The first reaction occurs quicker than the other and does not require a long curing time. For every other non fly ash C-based material, only the second described reaction takes place and a longer curing time is therefore required (see Table 8).

Table 12: Physical and mechanical properties of material made up of: fly ash C in SI units (A1) and standard units (A2); fly ash F in SI units (B1) and standard units (B2); bottom ash in SI units (C1) and standard units (C2)

Specimen	Specific Gravity	Compressive Modulus (GPa)	Compressive Strength (Mpa)
CC-7	1.52	0.64	10.19
CC-8	1.62	1.14	13.74
CC-9	1.64	0.93	14.45
CC-10	1.55	0.55	14.47
CC-11	1.52	0.69	11.24
CC-12	1.54	0.44	9.35

(A1)

Specimen	Specific Gravity	Compressive Modulus (ksi)	Compressive Strength (psi)
CC-7	1.52	93	1478
CC-8	1.62	165	1993
CC-9	1.64	135	2096
CC-10	1.55	79	2099
CC-11	1.52	100	1630
CC-12	1.54	64	1356

(A2)

Specimen	Specific Gravity	Compressive Modulus (GPa)	Compressive Strength (Mpa)
CF-7	1.17	0.83	11.03
CF-8	1.19	0.73	14.79
CF-9	1.31	1.65	24.43
CF-10	1.29	1.24	17.18
CF-11	1.31	1.54	24.03
CF-12	1.24	0.84	13.78

(B1)

Specimen	Specific Gravity	Compressive Modulus (ksi)	Compressive Strength (psi)
CF-7	1.17	120	1600
CF-8	1.19	106	2145
CF-9	1.31	239	3543
CF-10	1.29	180	2492
CF-11	1.31	223	3485
CF-12	1.24	122	1999

(B2)

Specimen	Specific Gravity	Compressive Modulus (GPa)	Compressive Strength (Mpa)
CB-7	0.96	0.82	3.06
CB-8	0.95	0.68	2.63
CB-9	0.95	1.01	3.18
CB-10	0.98	1.14	3.71
CB-11	1	1.04	2.97
CB-12	1	0.80	3.56

(C1)

Specimen	Specific Gravity	Compressive Modulus (ksi)	Compressive Strength (psi)
CB-7	0.96	119	444
CB-8	0.95	98	381
CB-9	0.95	147	461
CB-10	0.98	165	538
CB-11	1	151	431
CB-12	1	116	516

(C2)

When fly ash is used instead of cenospheres, both stiffness and strength of the materials increase along with the specific gravity of the material. Due to the fact that bottom ashes are mainly coarse aggregates, the CB-7 to CB-12 specimens have high porosity and have relative low density (0.95 to 1.0) compared to the density of bottom ash. If the compressive strengths of the bottom ash specimens are effectively similar to the CG500 and CG500 LF specimens, then the compressive modulus of the CB specimens are far higher (0.67 to 1.14 MPa). Table 13 summarizes all the results and compares the materials with other similar structural materials.

Table 13: Mechanical properties of the new materials and of three lightweight concretes in SI units (A1) and standard units (A2)

	Cenospheres	Fly Ash C	Fly Ash F	Bottom Ash	Autoclaved Aerated Concrete	Low-Density Cellular Concrete	Regular Cellular Concrete
Specific Gravity	0.45 - 0.65	1.5 - 1.65	1.2 - 1.3	0.95 - 1.0	0.5 - 0.85	0.3 - 0.8	0.8 - 1.92
Compressive Modulus (GPa)	0.4 - 0.9	0.4 - 1.1	0.7 - 1.7	0.7 - 1.1	1.35 - 2.6	0.2 - 2.2	1.1 - 14.3
Compressive Strength (MPa)	2.1 - 11.6	9.3 - 14.5	11 - 24.4	2.6 - 3.7	2.0 - 6.0	0.5 - 5.2	2.5 - 24.0

(A1)

	Cenospheres	Fly Ash C	Fly Ash F	Bottom Ash	Autoclaved Aerated Concrete	Low-Density Cellular Concrete	Regular Cellular Concrete
Specific Gravity	0.45 - 0.65	1.5 - 1.65	1.2 - 1.3	0.95 - 1.0	0.5 - 0.85	0.3 - 0.8	0.8 - 1.92
Compressive Modulus (ksi)	50 - 130	60 - 170	110 - 240	100 - 170	200 - 380	30 - 320	160 - 2070
Compressive Strength (psi)	310 - 1690	1360 - 2100	1600 - 3540	380 - 540	290 - 870	70 - 750	360 - 3480

(A2)

Influence of Curing Time

A material which can develop its maximum strength with an air setting at room temperature is highly appreciated in the construction field. Such a material requires less manufacturing utilities and can be cast in the field. If the material is not capable of an air setting at ambient temperature, there are other ways of achieving energy efficiency. One way of tackling this challenging problem is to decrease the curing time or curing temperature. To do so, aluminum phosphate can be added to the mixture. Aluminum phosphate is a white, crystalline powder which, in everyday' life, can be used as a leavening agent but its dehydrating agent properties make it suitable for some industrial applications. When heated, aluminum phosphate decomposes into aluminum oxide and phosphorus pentoxide. The latter is the compound having good moisture absorption properties.

Aluminum phosphate has already been used in prior research with the aim of decreasing curing time. In the past, a high strength mortar capable of air setting at room

temperature (Greger, 1943) came out of such research. The problem with refractory mortar, which consists in a mix of filler (ceramic grog), bond clay and some water, is that it requires a high temperature for the bond to be strong. This discovery tackles this issue by processing the ceramic filler with a water soluble aluminum phosphate before the addition of the bond clay. Other inventions based on aluminum phosphate have a direct application in the automotive industry. It is the case of a high temperature heat-insulating structure based on an aqueous aluminum phosphate solution with foamable perlite particles (filler) which is essentially chemically composed of silica (70-75%) and alumina (12-15%) (Noda and Takeuchi, 1974). This material can be applied to the area around the exhaust pipe which is under conditions of high heat and high stress. Mix compositions containing a relatively high percentage of alumina bound chemically by aluminum phosphate are well known in the art. In particular, a new refractory material based on magnesium oxide, aluminum phosphate and an insulating filler which demonstrates excellent temperature resistance and good strength has been patented (Salazar, 1982). More recently, a cement containing magnesium oxide and aluminum phosphate able to harden quickly - less than one hour - and allowing people to repair some damages requiring immediate intervention (such as a hole on the highway), has been developed and patented (Tomic, 1982). A balance between working time and curing time is found by controlling the proportions of magnesium oxide, aluminum phosphate and inert aggregates. The chemical reaction between aluminum phosphate and fly ash has some cementitious properties which have already been applied to increase the compressive strength of rapid-setting concrete based on magnesium oxide and aluminum phosphate (Tomic, 1986). Two materials have finally emerged from this research: one rapid setting composition having a work time of ten minutes at least and a hard, concrete-like product, based on the same components, having a compressive strength of at least 20 MPa.

Earlier investigations on the material have demonstrated that the strength of the material increases with curing time before reaching a plateau (Biju-Duval, 2007).

However, the following investigation reveals that a significant amount of strength can be gained for low curing time by adding some aluminum phosphate to the mixture. To highlight the influence of the aluminum phosphate, different quantities of a 62.5g/L solution aluminum phosphate (0mL, 8mL, 12mL) have been added to CG106-9 specimen. This experimental protocol has been repeated with four different curing times (1h, 2.5h, 4h and 5.5h). The Strength vs. Aluminum Phosphate Quantity curves for each curing time are shown below (Fig.12):

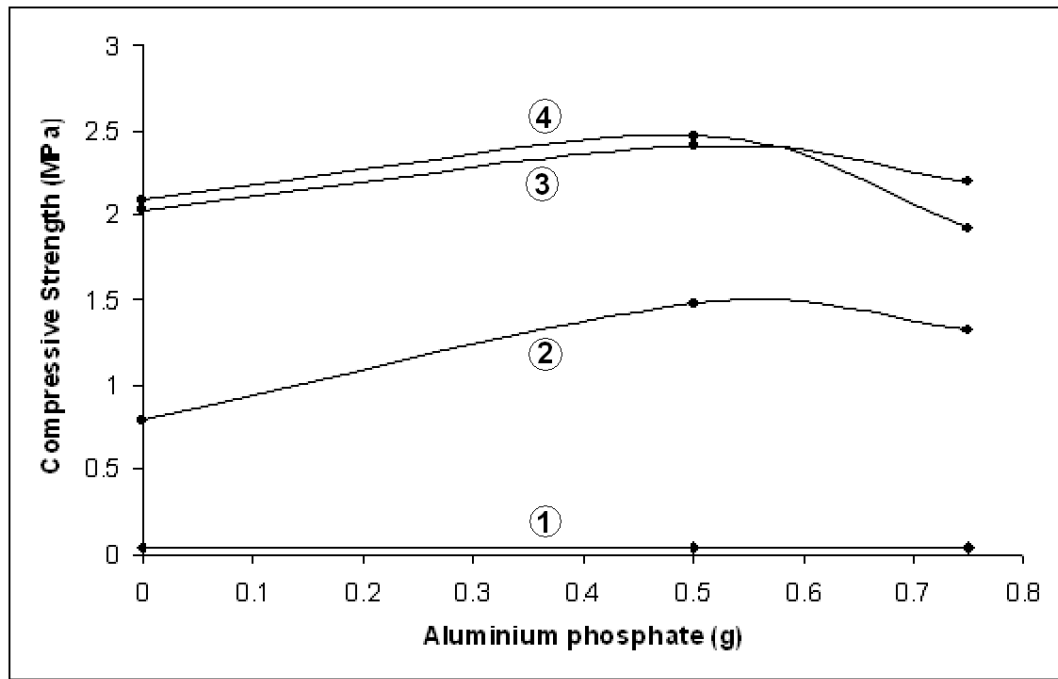


Figure 12: Strength vs. Aluminum phosphate quantity for CG106-9 after a curing of: (1) 1h; (2) 2.5h; (3) 4h; (4) 5.5h

Each curve exhibits a first positive slope corresponding to an increase of strength along with the increasing quantities of aluminum phosphate. Then, for each curing time, we can observe a decrease of the strength for higher concentrations of aluminum phosphate. An optimal quantity of aluminum phosphate, leading to a maximum strength,

therefore exists. Added in small quantity, aluminum phosphate absorbs the moisture and allows the material to reach a higher strength in less time. However, experiments have revealed that significant amounts of aluminum phosphate (more than 1 gram) alter the quality of the material's bond and decrease its strength. Below are summarized the compressive strength improvements reached with the addition of aluminum phosphate (Table 14). Since aluminum phosphate does not allow the materials to reach sufficient strength for structural applications, this analysis has only an enlightening aspect and does not provide any solid evidence of a potential application for aluminum phosphate.

Table 14: Compressive strength increase due to the addition of 0.5g of aluminum phosphate for CG106-9 after 1h, 2.5h, 4h and 5.5h of curing

	Aluminum Phosphate		
	0g	0.5g	
Curing Time	Compressive Strength (MPa)		Compressive Strength Increase
1h	0.04	0.042	5.00%
2.5h	0.79	1.48	87.34%
4h	2.03	2.41	18.72%
5.5h	2.09	2.47	18.18%

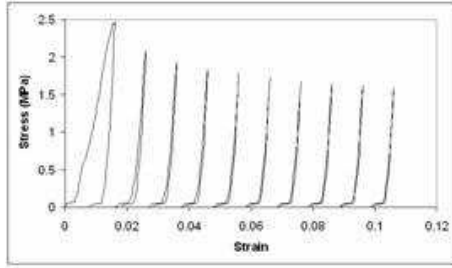
CHAPTER 4

CONCLUSIONS

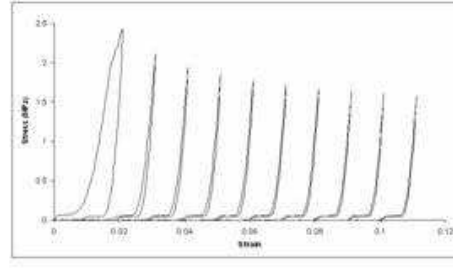
The building and construction industry is looking for a generation of non-cement materials to replace or reduce the utilization of concrete. This thesis presents ongoing work on a new series of materials based on Coal Combustion Products (CCP) that also do not contain cement. The thesis reported on the specific gravities, as well as the corresponding compressive strength and modulus. It was found that these materials can acquire compressive strengths as high as 3,600 psi making them stronger than conventional and lightweight concrete at modest specific gravities ranging from 0.5 to 1.6. Indeed, these materials present an opportunity to convert an unwanted CCP byproduct into a commercially attractive raw material; and it will certainly help increase the utilization of CCP while reducing the use of concrete and timber in many applications. While these materials are cured between 3 and 24 hours at 90 to 115 degrees Celsius, some investigations were conducted on chemical additives that can reduce the curing time. One such additive included aluminum phosphate, but it is not conclusive at this time whether this additive is helpful or not. Curing times as well as reinforcement are proposed as subjects for further work on these materials.

APPENDIX

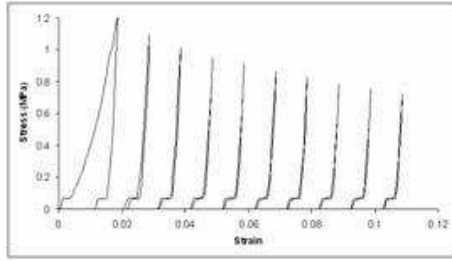
STRESS-STRAIN CURVES IN ELASTIC RANGE



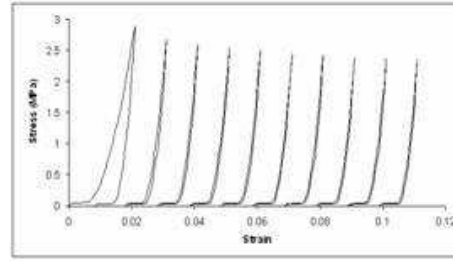
(a)



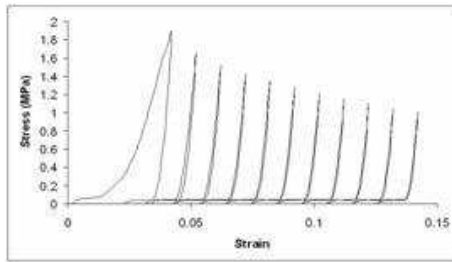
(b)



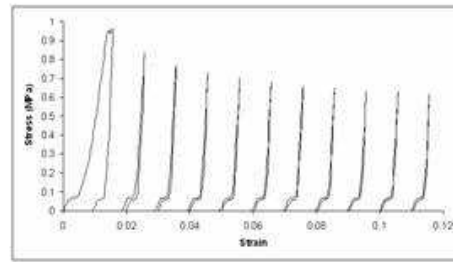
(c)



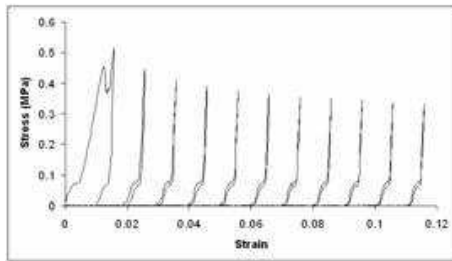
(d)



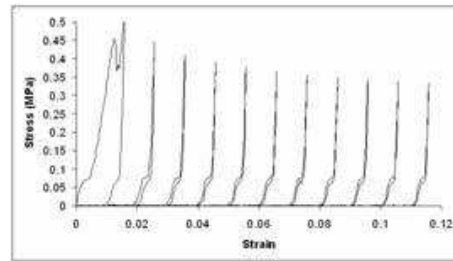
(e)



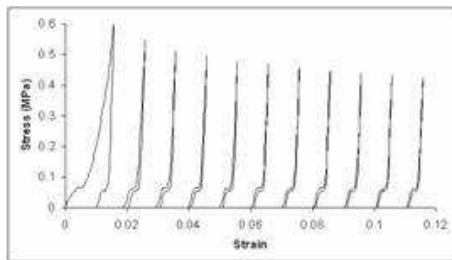
(f)



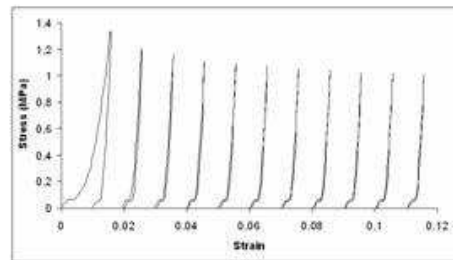
(g)



(h)

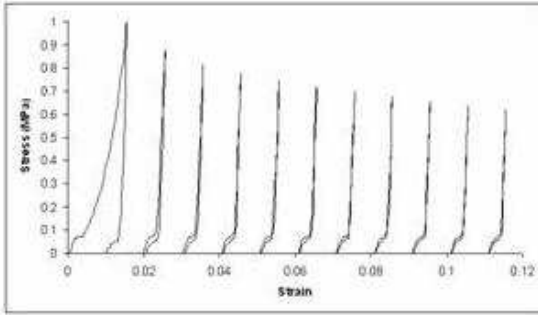


(i)

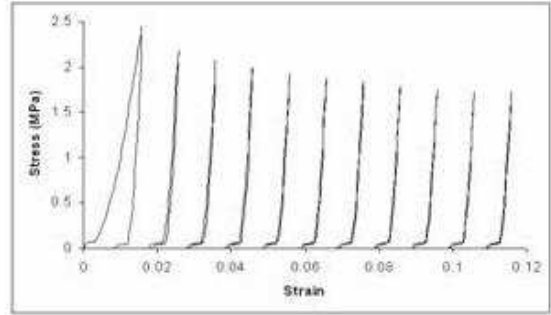


(j)

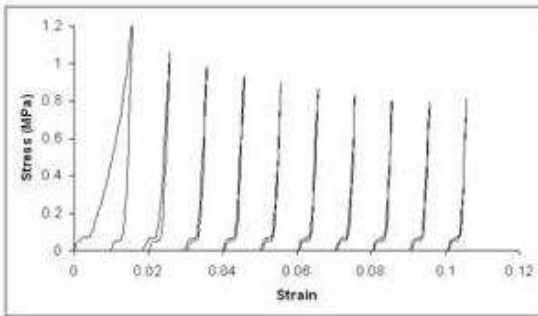
Stress-strain curves in elastic range for: (a) CG500-1; (b) CG500-2; (c) CG500-3; (d) CG500-4; (e) CG500-7; (f) CG500-8; (g) CG500-9; (h) CG500-10; (i) CG500-11; (j) CG500-12



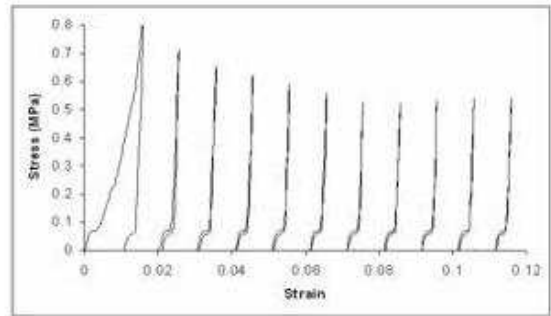
(a)



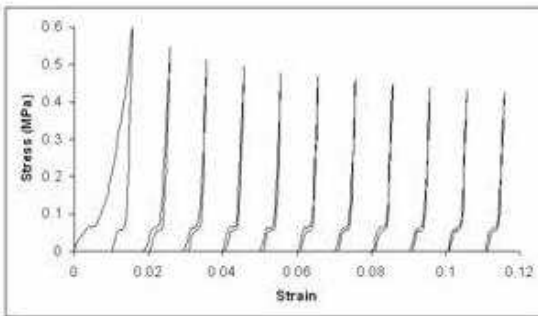
(b)



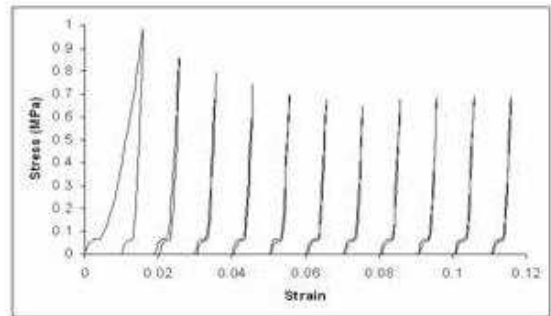
(c)



(d)

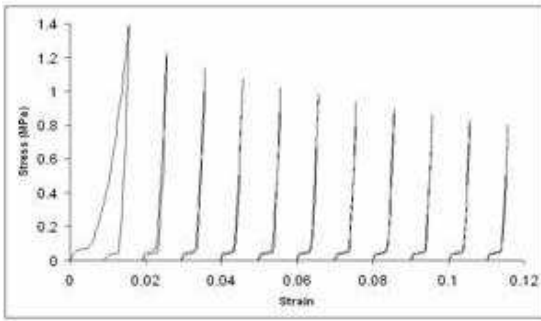


(e)

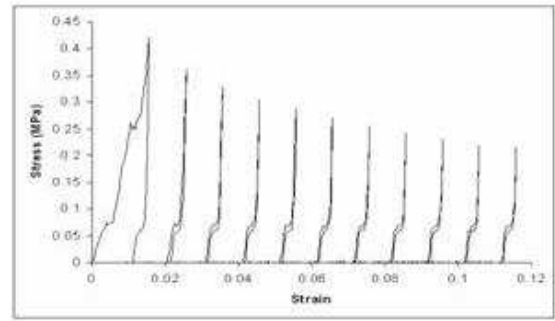


(f)

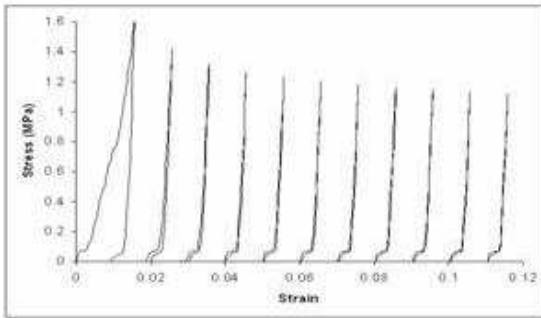
Stress-strain curves in elastic range for: (a) CG500LF-7; (b) CG500LF-8; (c) CG500LF-9; (d) CG500LF-10; (e) CG500LF-11; (f) CG500LF-12



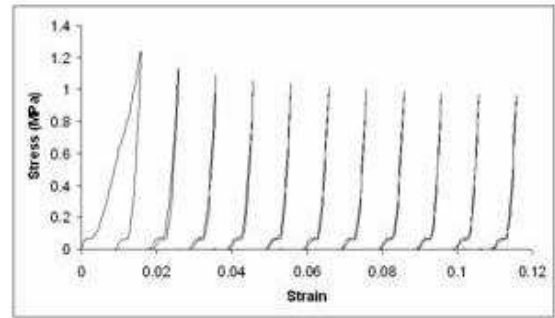
(a)



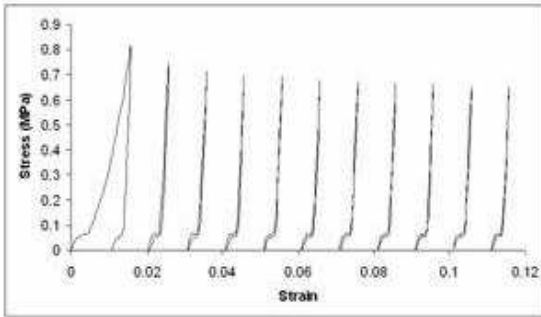
(b)



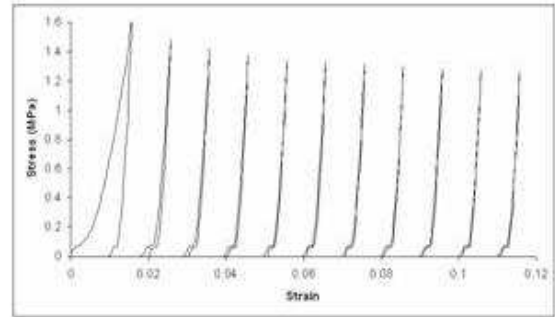
(c)



(d)

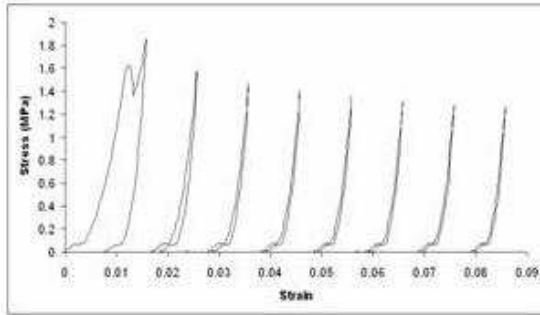


(e)

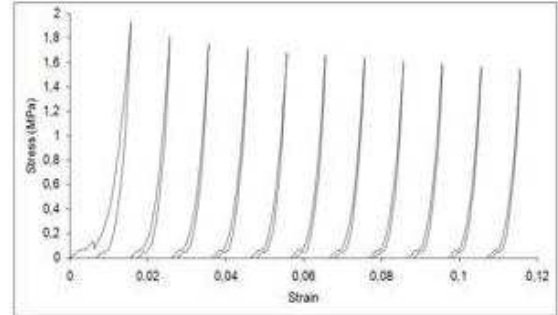


(f)

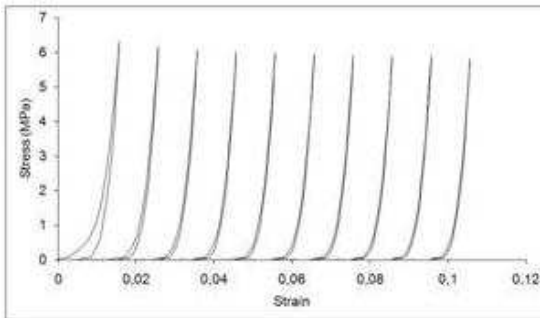
Stress-strain curves in elastic range for: (a) CG106-7; (b) CG106-8;
(c) CG106-9; (d) CG106-10; (e) CG106-11; (f) CG106-12



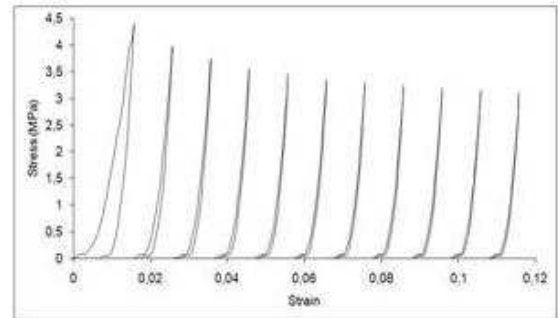
(a)



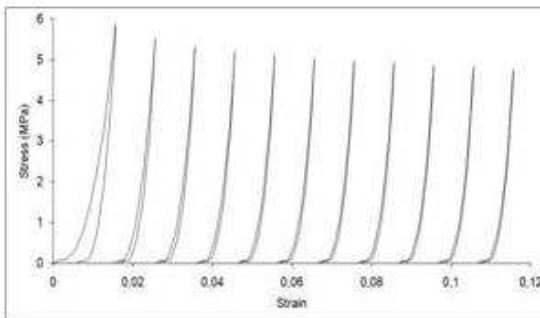
(b)



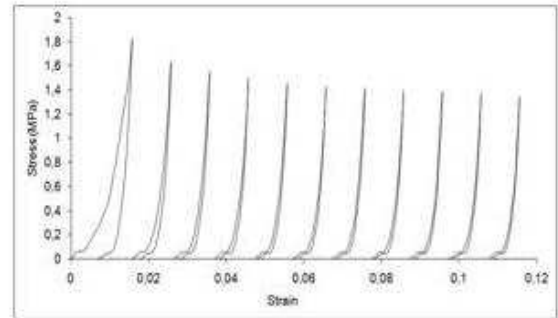
(c)



(d)

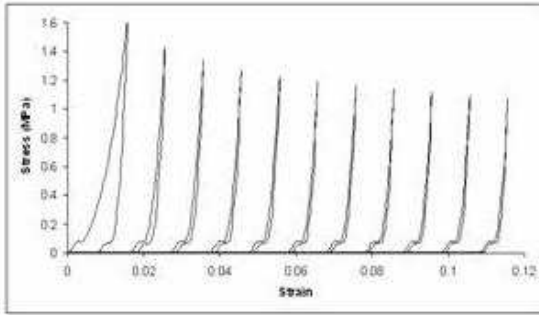


(e)

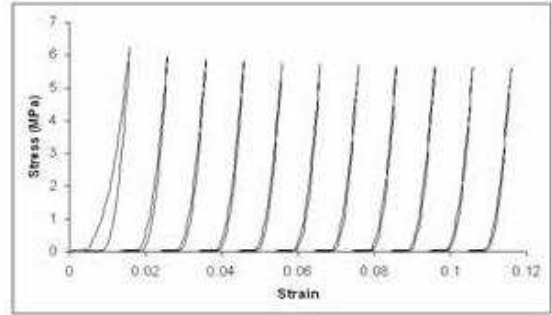


(f)

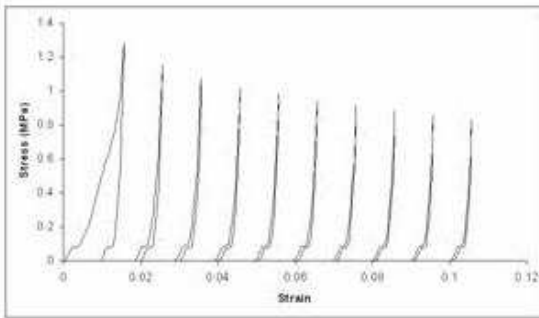
Stress-strain curves in elastic range for: (a) CC-7; (b) CC-8;
(c) CC-9; (d) CC-10; (e) CC-11; (f) CC-12



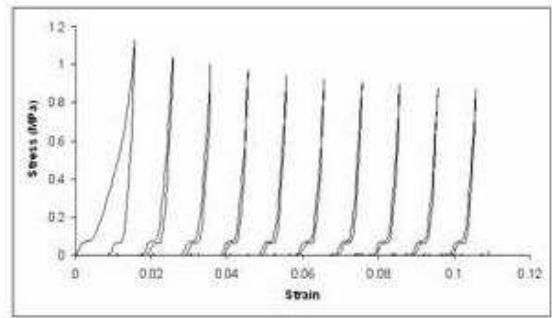
(a)



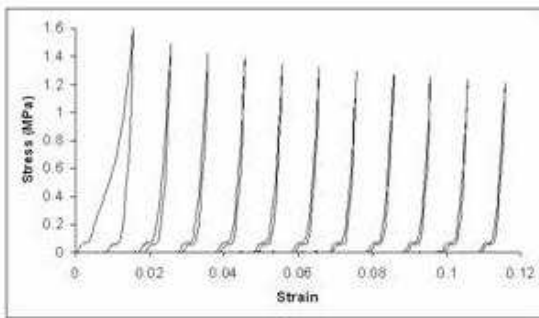
(b)



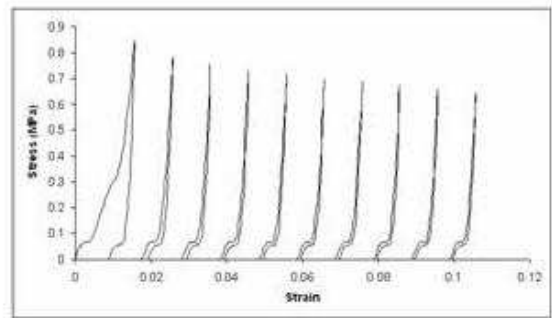
(c)



(d)

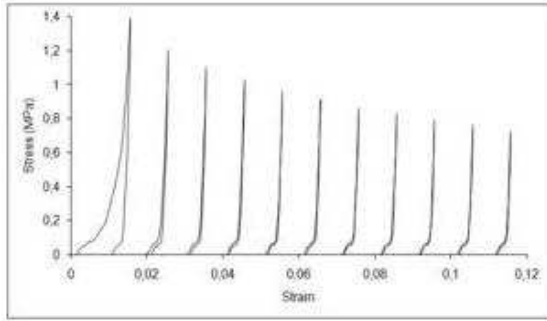


(e)

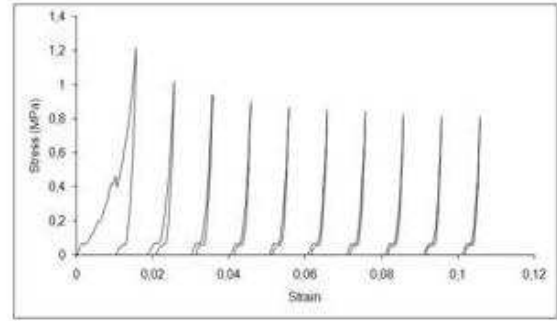


(f)

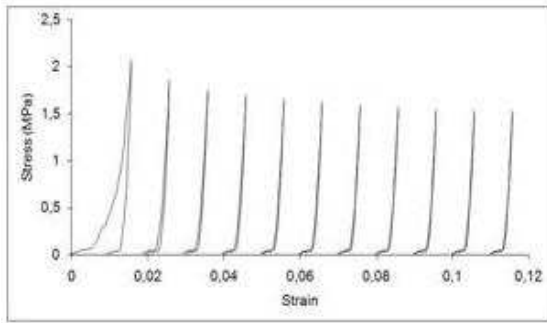
Stress-strain curves in elastic range for: (a) CF-7; (b) CF-8;
(c) CF-9; (d) CF-10; (e) CF-11; (f) CF-12



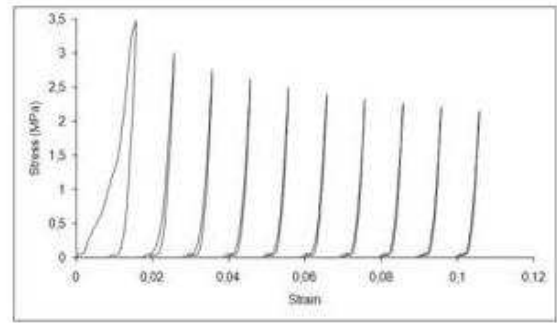
(a)



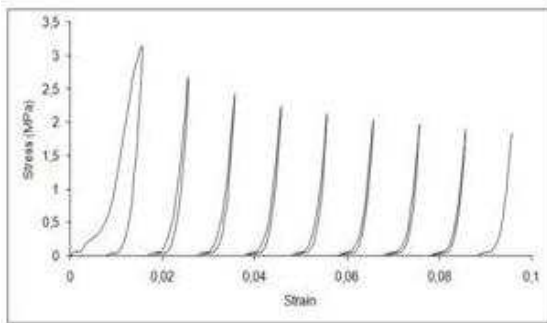
(b)



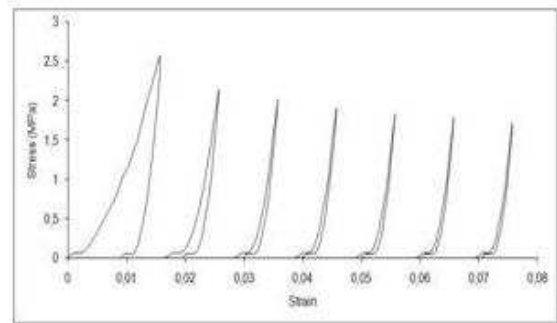
(c)



(d)



(e)



(f)

Stress-strain curves in elastic range for: (a) CB-7; (b) CB-8;
(c) CB-9; (d) CB-10; (e) CB-11; (f) CB-12

REFERENCES

- ACI 523.1R-06, Guide for Cast-in-Place Low-Density Cellular Concrete, ACI Committee 523, 4-6 (2006)
- ACI 530.1-08, Building Code Requirements and Specification for Masonry Structures and Related Commentaries, ACI Committee 530 (2008)
- ACI Board Advisory Committee on Sustainable Development, White Paper on Sustainable Development, Concrete International, American Concrete Institute, 27, 2, 19-21 (2005)
- American Coal Ash Association (ACAA), CCP Production and Use Survey (2006)
- ASTM C618-08a, Standard Specification for Coal Fly Ash and Raw or Calcined Natural Pozzolan for Use in Concrete, C09.24 Subcommittee (2008)
- Biju-Duval P, A New Porous Material Based on Cenospheres, Georgia Institute of Technology ETD (2007)
- European Coal Combustion Products Association (ECOBA), CCP Production & Use Survey (EU 15)(2003)
- Fatih T., and Ümit A., Utilization of Fly Ash in Manufacturing of Building Bricks, 2001 International Ash Utilization Symposium, Center for Applied Energy Research, University of Kentucky, Paper # 13 (2001)
- Fearnside P.M., and W.F. Laurance, Tropical deforestation and greenhouse-gas emissions, Ecological Applications, 14, 4, 982–986 (2004)
- Greger H.H., Method of preparing air-setting refractory mortars, United States Patent 2425151 (1943)
- Hebel, Hebel AAC Products and How to Work with Them, HEBEL International Tech Manual, Section 2 (1997)

- Legatsi L.A., Cellular Concrete, ASTM STP169C-EB, Significance of Tests and Properties of Concrete and Concrete-Making Materials, 533-539 (1994)
- Liu H., Method to produce durable non-vitrified fly ash bricks and blocks, Patent filed with the Bureau of Intellectual Property Rights of the People's Republic of China, Patent Application No. 200680000117.3 (2007)
- Malhotra V.M., Reducing CO₂ Emissions, Concrete International, American Concrete Institute, 28, 9, 42-45 (2006)
- Mehta P.K., Coal fly ash: the most powerful tool for sustainability of the concrete industry, Ash at Work; Journal Issue: 1 (2008)
- Moran, E.F., Deforestation and Land Use in the Brazilian Amazon, Human Ecology, 21, 1 (1993)
- Mukherjee A. B., and R. Zevenhoven, Mercury in coal ash and its fate in the Indian subcontinent: A synoptic review , Science of The Total Environment, 368, 1, 384-392 (2006)
- Natesan M., S. Smith and K. Humphreys, The Cement Industry and Global Climate Change: Current and Potential Future Cement Industry CO₂ Emissions, 6th International Conference on Greenhouse Gas Control Technologies, 995-1000 (2002)
- Noda F, and Takeuchi Y., High temperature heat-insulating structure, United States Patent 3958582 (1974)
- Paul W. L. and P. A. Taylor, A comparison of occupant comfort and satisfaction between a green building and a conventional building, Building and Environment, 43, 1858–1870 (2008)
- Ries R. and M. M. Bilec, The economic benefits of green buildings: a comprehensive case study, The Engineering Economist, 51, 259–295 (2006)
- Salazar P.V., Refractory compositions and methods, United States Patent 4432799 (1982)

Singhal G.S., G. Renger, S.K. Sopory, K.D. Irrgang and Govindjee, The Photosynthetic Process, Concepts in Photobiology: Photosynthesis and Photomorphogenesis, 11-51 (2006)

South African Coal Ash Association (SACAA)

Tanyildizi H. and A. Coskun, Performance of lightweight concrete with silica fume after high temperature, Construction and Building Materials, 22, 10, 2124-2129 (2008)

Tomic E.A., Phosphate cement and mortar, United States Patent 4394174 (1982)

Tomic E. A., Phosphate cement including fly ash for high-strength concrete-like products, United States Patent 4749413 (1986)

World Business Council for Sustainable Development, The Cement Sustainability Initiative (2002)

WWF Indonesia Technical Report, Deforestation, Forest Degradation, Biodiversity Loss and CO₂ Emissions in Riau, Sumatra, Indonesia (2008)

Yazıcı H., H. Yigiter, A. S. Karabulut and B. Baradan, Utilization of fly ash and ground granulated blast furnace slag as an alternative silica source in reactive powder concrete, Fuel, 87, 12, 2401-2407 (2008)